Ultrasound in Med. & Biol., Vol. 41, No. 5, pp. 1311–1319, 2015

0301-5629/$ - see front matter

http://dx.doi.org/10.1016/j.ultrasmedbio.2014.12.008

● *Original Contribution*

MEASUREMENT OF INTERNAL DIAMETER CHANGES AND PULSE WAVE VELOCITY IN FETAL DESCENDING AORTA USING THE ULTRASONIC PHASED-TRACKING METHOD IN NORMAL AND GROWTH-RESTRICTED FETUSES

Susumu Miyashita,*† Jun Murotsuki,*† Jin Muromoto,*† Katsusuke Ozawa,*† Nobuo Yaegashi,‡ Hideyuki Hasegawa,§ and Hiroshi Kanai§

*Department of Advanced Fetal and Developmental Medicine, Tohoku University Graduate School of Medicine, Sendai, Miyagi, Japan; †Department of Maternal and Fetal Medicine, Miyagi Children's Hospital, Sendai, Miyagi, Japan; ‡Department of Obstetrics and Gynecology, Tohoku University, Sendai, Miyagi, Japan; and §Department of Electronic Engineering, Tohoku University Graduate School of Engineering, Sendai, Miyagi, Japan

(*Received* 21 *January* 2014; *revised* 7 *December* 2014; *in final form* 11 *December* 2014)

Abstract—Phased tracking (PT) is an ultrasound-based technique that enables precise measurement of a target velocity. The aims of this study were to use PT to evaluate arterial pulse waveform, pulse wave velocity and fetal pulse pressure in normal and growth-restricted fetuses. One hundred fetuses with normal development and 15 fetuses with growth restriction were analyzed. Ultrasonic raw radiofrequency signals were captured from a direction perpendicular to the vascular axis at the fetal diaphragmatic level for the difference in internal dimensions (DID), or simultaneously from different directions for the pulse wave velocity. Pulsatile movement of the proximal and distal intima of the vessels was analyzed using PT. The fetal DID exhibited no significant changes in growth-restricted fetuses. Pulse wave velocity (3.8 ± 0.32 m/s vs. 2.2 ± 0.069 m/s, $p < 0.001$) and estimated pulse pressure (6.9 ± 0.90 kPa vs. 2.5 ± 0.18 kPa, $p < 0.001$) were significantly elevated in growth-restricted fetuses. Assessment of DID and pulse wave velocity of the descending aorta using PT is a feasible, non-invasive approach to evaluation of fetal hemodynamics. (E-mail: ssmu.miyashita@nifty.ne.jp) © **2015 World Federation for Ultrasound in Medicine & Biology.**

Key Words: **Phased-tracking method, Pulse wave velocity, Fetal pulse pressure, Fetal growth restriction.**

INTRODUCTION

Recent developments in high-resolution ultrasound systems have enabled the precise observation of fetal organs at an early gestational age. However, the measurement of very small structures and their fine movements remains a formidable challenge, because of the various physical properties (*e.g.*, transmitting ultrasonic frequency or wavelength) that limit measurement accuracy. In particular, conventional diagnostic ultrasound systems have difficulty measuring small displacements less than the wavelength; this has prevented examiners from measuring the fine motion of objects such as the fetal vessel wall.

Hokanson et al. (1970, 1972) developed a phase-locked echo-tracking system that enables the assessment of arterial wall motion using phase-related tracking gates. Several studies have employed a phase-locked echo-tracking system to examine fetal vascular pulsation (Gennser and Isberg 1987; Luterkort and Gennser 1987; Mori et al. 2000; Sindberg Eriksen and Gennser 1984; Stale et al. 1991; Struijk et al. 1992), and Fujita et al. (2002) reported a linear relationship between the pressure and internal diameter of the fetal descending aorta in an animal model. Of note, a more recent echo-tracking system can measure arterial internal diameter changes within one-sixteenth of the ultrasound wavelength used by an instrument (*e.g.*, a precision of approximately 20 μm with a transmission frequency of 5 MHz) (Niki et al. 2002). Struijk et al. (2013) published a study on assessment of fetal pulse pressure using the echo-tracking system.

Kanai et al. (1996) developed another ultrasonic tracking system called the phased-tracking (PT) method,

Address correspondence to: Susumu Miyashita, Miyagi Children's Hospital, 4-3-17, Ochiai, Aoba borough, Sendai City, Miyagi, Japan 989-3126. E-mail: ssmu.miyashita@nifty.ne.jp

Conflicts of interest: The authors have no conflicts of interest to declare.

which uses small phase differences in raw radiofrequency (RF) signals to obtain measurements. Accurate tracing and a very high spatial resolution of 0.5 μm can be achieved when PT is used to evaluate fine movements. Further, the simultaneous recording of RF signals from different beam directions would hypothetically allow evaluation of fetal pulse wave velocity (PWV). However, to date, no study has evaluated fetal PWV while using PT. Because these parameters allow the estimation of fetal pulse pressure (PP), their accurate measurement is essential for understanding hemodynamic alterations, especially in compromised fetuses.

Recent study revealed histologic changes and deteriorated compliance in the arterial walls in growth-restricted fetuses of animal model (Dodson et al. 2013). Here, the study aims were to evaluate fetal arterial pulse waveform and PWV and to estimate fetal blood pressure and changes in growth-restricted fetuses using PT.

METHODS

Patients

One hundred fifteen women with singleton pregnancies were enrolled in this study. One hundred fetuses (16–40 wk of age) exhibited normal growth, and 15 (24–34 wk of age) were growth restricted. Fetuses with apparent fetal anomalies, including structural heart disease, arrhythmia, hydrops, macrosomia, multiple pregnancy, chromosomal abnormalities and congenital infection and fetuses of mothers with complications such as diabetes, anemia, drug abuse, alcoholic/smoking history, hypertension and significant heart/liver/renal disease were excluded from the study. This study was approved by the institutional ethics committee, and all measurements were performed with written informed consent at the Department of Maternal and Fetal Medicine of Miyagi Children's Hospital, Sendai City, Japan, from June 2010 to May 2013. A fetus was defined as growth restricted when the *Z*-score of the estimated weight was equal to or less than −1.5 SD of the Japanese standard. No repeated measurements were performed in any of the cases during the gestational period. Table 1 lists the characteristics of the patients.

Table 1. Characteristics of the patients

	Normal fetuses	Growth-restricted fetuses	*p*-value
Number of fetuses analyzed	100	15	
Number of fetuses with available data			
Pulse waveform	97	15	
Pulse wave velocity	65	15	
Estimated fetal pulse pressure	54	15	
Fetal age at measurement (wk)	27.5 ± 6.3*	31.0 ± 5.6	0.099
Maternal age	30.1 ± 4.6	30.3 ± 5.4	0.78
Nulliparous	38	9	0.092
Maternal pre-eclampsia	0	0	—
Non-reassuring fetal status	0	0	—
Oligohydramnios	0	1	0.13
AEDV in umbilical artery	0	1	0.13
CPR < 1	0	3	0.0018

AEDV = absent end-diastolic velocity; CPR = cerebroplacental ratio in the Doppler examination.
* Mean ± standard deviation.

Ultrasonic phased-tracking method

With the use of ultrasonic diagnostic equipment (Hitachi-ALOKA ProSound F75, Tokyo, Japan), the direction of the ultrasonic beam was fixed, and the received RF signals were sampled at 20 MHz for several cardiac cycles. Quadrature demodulation was applied to the sampled RF signals off-line. The principles underlying PT, including theoretical and *in vivo* evaluations of the measurements, have been described previously (Kanai et al. 1996).

Radiofrequency pulses with an angular frequency of $\omega_0 = 2\pi f_0$ (f_0 = 5 MHz) are transmitted at time intervals of ΔT. The phase difference, $\Delta\theta(x; t)$, between the phase $\theta(x; t)$ of the quadrature-demodulated signal $z(x; t)$ of the received signal, $y(x; t)$, and the phase $\theta(x; t + \Delta T)$ of the quadrature-demodulated signal $z(x; t + \Delta T)$ of the subsequently received signal, $y(x; t + \Delta T)$, is given by

$$\Delta\theta(x;t) = \theta(x;t+\Delta T) - \theta(x;t) = -\frac{2\omega_0}{c_0}\cdot\Delta x(t) \qquad (1)$$

where $\Delta x(t) = x(t + \Delta T) - x(t)$ is the movement of the object during the short period ΔT around time t, and c_0 is the acoustic velocity in the soft tissue.

In the present study, ΔT was set at 2.38 ms. That is, the frame rate was 421 Hz, so that the measurable velocity was set at a fair limit of 0.32 m/s (at f_0 = 5 MHz). By dividing the movement Δx by the period ΔT, the average velocity $v(t + \Delta T/2)$ of the object during the period ΔT is given by

$$v\left(t+\frac{\Delta T}{2}\right) = \frac{\Delta x(t)}{\Delta T} = \frac{c_0}{2\omega_0}\cdot\frac{\Delta\theta(x;t)}{\Delta T} \qquad (2)$$

The phase difference $\Delta\theta(x; t)$ is accurately determined by the constrained least-squares approach based on the complex cross-correlation between $z(x; t)$ and $z(x; t + \Delta T)$ under the condition that signal waveforms change only in phase values during ΔT. It is impossible to accurately determine the true lag value from the complex correlation function, which is derived from the standard normalized mean squared difference between the quadrature-modulated signals of the successively received signals (Sabbah et al. 1981). However, the introduction of the constraint is effective for determining the

lag between these complex signals. By multiplying the resultant velocity $v(t + \Delta T/2)$ by ΔT, the next depth $x(t + \Delta T)$ of the object is estimated as

$$\Delta x(t+\Delta T) = x(t)+\mathrm{v}\left(t+\frac{\Delta T}{2}\right)\cdot \Delta T \qquad (3)$$

With the estimated depth position $x(t + \Delta T)$, the position of the region of interest on the vessel wall is successfully tracked. The initial positions of the sampling points on the vessel wall were manually set along the ultrasonic beam.

In this study, a high-speed analogue-to-digital converter with large-scale memory was employed to analyze the complex signal resulting from the quadrature modulation of the signal received by a 5-MHz convex-type ultrasonic transducer connected to standard ultrasonic diagnostic equipment. The lower limit of resolution of vessel wall displacement was 0.5 μm, and the higher limit of measurable velocity was about 0.32 m/s, which was determined by aliasing of the conventional Doppler system.

Pulse waveforms of the dimensions of the descending aorta

The fetal descending aorta was identified in the longitudinal direction on the transabdominal B-mode plane using a 5-MHz convex matrix-array probe. RF signals were captured for 2 to 4 s from an adjusted beam direction perpendicular to the arterial axis at the level of the diaphragm (Fig. 1). PT was employed for off-line analysis of pulsatile movement of the proximal or distal border of the arterial lumen, which was assumed to be the intima of the vessels, and the initial positions for tracking were indicated manually using a mouse. The velocities of the proximal or distal border could be analyzed as primary data, and the differential between these parameters implied the velocity of the changes in internal dimensions, whereas the time integral of these parameters revealed changes in internal diameter. On the basis of this analysis, we evaluated the following parameters: V_s, the maximum velocity in the systolic phase; V_d, the minimum velocity in the diastolic phase; D_{max}, the maximum internal diameter in the systolic phase; and D_{min}, the minimum internal diameter in the diastolic phase. The difference in internal dimensions (DID) was obtained from the differential between D_{max} and D_{min}. All measurements were performed in resting fetuses; background fetal motion, such as breathing movements, were avoided. The averages of five cardiac cycles were analyzed. Figure 2 illustrates an example of the analyzed waves of a changing velocity and the displacement of an internal diameter.

Pulse wave velocity

At the same setting used for measuring the dimensions of the descending aorta, RF signals were captured simultaneously from different directions. PT was applied to the proximal border of the lumen at different positions in the descending aorta. A measuring point was set on the

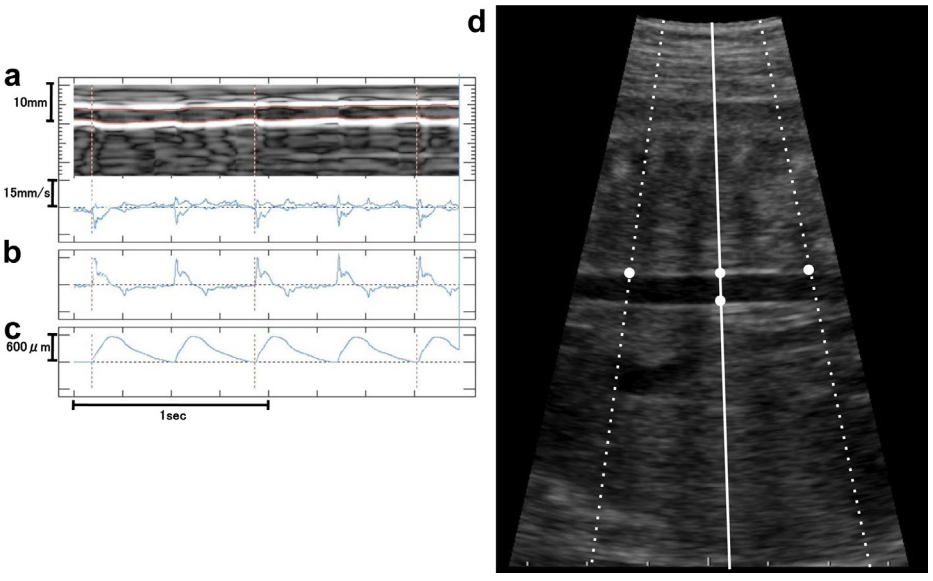

Fig. 1. Analysis of pulse waveforms for the dimensions of the fetal descending aorta. (a) Each velocity of the proximal and distal border of the lumen was analyzed using the phased-tracking method (PT). (b) Differences between the two waves in (a) were used to determine the velocity of the change in internal diameter. (c) The time integral of the wave in (b) yielded the change in internal diameter. (d) The direction of the beam transmission was set perpendicular to the arterial axis at the level of the diaphragm.

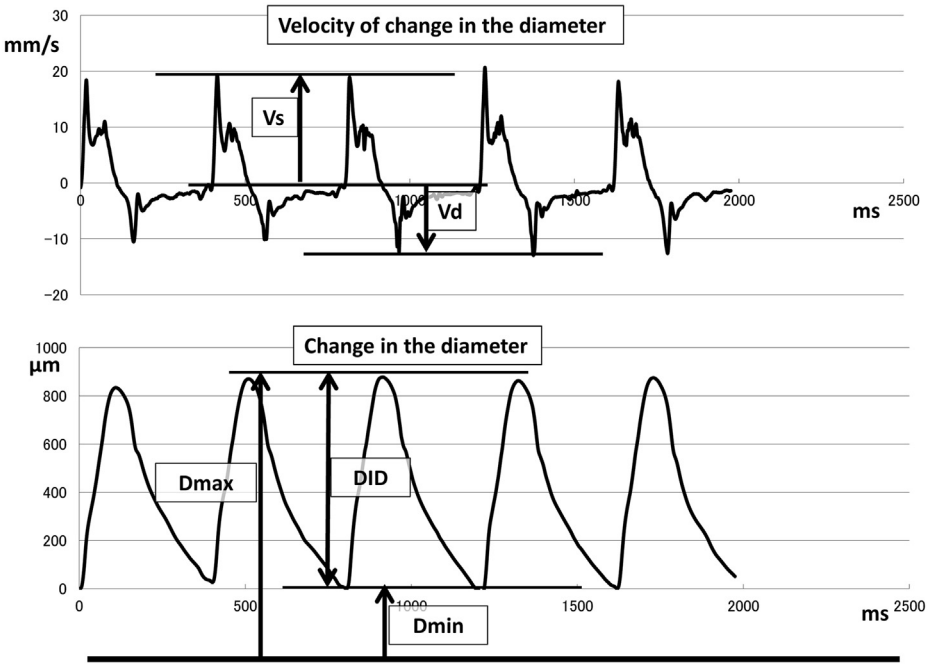

Fig. 2. Definitions of the parameters analyzed in this study. V_s = maximum velocity in systolic phase; V_d = minimum velocity in diastolic phase; D_{max} = maximum internal diameter in systolic phase; D_{min} = minimum internal diameter in diastolic phase; DID = difference in internal dimensions.

upper side of the diaphragm, and another on the lower side (Fig. 3). The velocities of the proximal border were analyzed at each position, and the time delay between them was measured; the average of five cardiac cycles was used for the analysis. PWV was obtained by dividing the distance between the analyzed positions by the time delay of the pulse wave. The time delay in the velocity waves of the arterial wall was analyzed and defined as the peak-to-peak interval in the systolic phase.

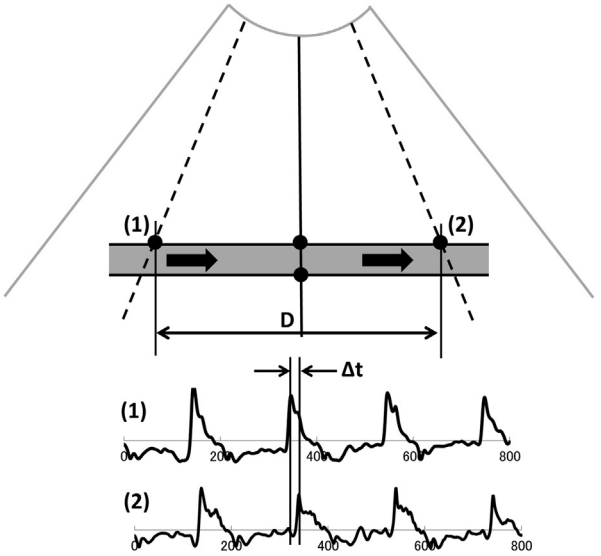

Fig. 3. Analysis of pulse wave velocity (PWV) for the fetal descending aorta. Radiofrequency signals were captured simultaneously from different directions. The velocity of the proximal border of the lumen at different positions on the descending aorta was analyzed with the phased-tracking method. PWV was obtained by dividing the distance between the analyzed points (D) by the delayed time (Δt) of the velocity wave.

Estimation of fetal pulse pressure

In the Moens–Korteweg equation, PWV (m/s) is given by

$$\mathrm{PWV} = \sqrt{\frac{E_\theta h}{\rho d}} \tag{4}$$

where E_θ is the circumferential elastic modulus of the wall, h is the wall thickness, d is the internal diameter and ρ is the blood density. The elastic modulus was defined as the ratio of circumferential wall stress to strain and is given by

$$E_\theta = \frac{\text{stress}}{\text{strain}} = \frac{(d/2h)\Delta p}{(\pi(d+\Delta d)-\pi d)/\pi d} = \frac{d^2}{2h\Delta d}\Delta p \tag{5}$$

where Δd is the difference in internal diameter, and Δp is the PP. Substitution of E_θ in (5) with (4) yields

$$\mathrm{PWV} = \sqrt{\frac{E_\theta h}{\rho d}} = \sqrt{\frac{d\Delta p}{2\rho\Delta d}} \tag{6}$$

The PP (Δp [N/m^2]) can be estimated as

$$\Delta p = \frac{2\rho\Delta d}{d}\cdot \mathrm{PWV}^2 \quad (7)$$

Statistical analysis

All measured data were analyzed using JMP 10.0.2 (SAS, Cary, NC, USA, 2013) or R 2.6.2 (The R Foundation for Statistical Computing, 2012). Both linear and non-linear regression analyses were applied to the building of regression models. Fisher's exact test, the Mann–Whitney *U*-test and two-way factorial analysis of variance (ANOVA) were employed to compare growth-restricted fetuses with normally growing fetuses through gestation. We verified intra-observer variability with the coefficient of variation (CV) and intra-class correlation coefficient (ICC) of repeated measurements (68 cases for pulse waveforms of dimensions and 53 cases for PWV). There were only two ultrasound observers in this study. Inter-observer variability was also examined using Bland–Altman analysis of alternate measurements in two cases of normal development for 28 wk. Statistical significance was set at $p < 0.05$.

RESULTS

Pulse waveforms of the dimensions of the descending aorta

Data for 97 of the 100 normal fetuses and all of the growth-restricted fetuses were available for analysis; data for 3 normal fetuses were excluded because of poor recording. Analysis of the measurements by gestational week is illustrated in Figure 4(a, b). Table 2 summarizes the results of the regression analyses for each parameter evaluated.

Pulse wave velocity

After the exclusion of data for 32 normal fetuses because of poor recordings or missed measurements, data for 65 normal fetuses and all growth-restricted fetuses were available for analysis. Fetal PWV by gestational week is illustrated in Figure 5 for the two study groups. Results of regression analyses for the normal and growth-restricted fetuses are summarized in Table 2. PWV of the descending aorta was significantly higher in growth-restricted fetuses compared with normal fetuses (mean ± standard error: 3.8 ± 0.32 m/s vs. 2.2 ± 0.069 m/s, $p < 0.001$).

Estimated fetal pulse pressure

Measurements for 54 normal fetuses and all growth-restricted fetuses were available for estimating fetal PP (Fig. 6). It was possible to estimate fetal PP with eqn (7) using DID/D_{min} and PWV when the blood density was set at 1.05 (Hinghofer-Szalkay and Greenleaf 1987). Estimated PP was significantly elevated in growth-restricted fetuses (6.9 ± 0.90 kPa vs. 2.5 ± 0.18 kPa, $p < 0.001$).

Intra-observer and inter-observer variability

The CV, ICC and Bland–Altman analysis of measurements are summarized in Table 3. The CV was less than 10% overall for the parameters analyzed, and there was no specific tendency toward a change in the evaluation during the gestational period. Bland–Altman analysis revealed no significant differences between observers.

DISCUSSION

Pulse waveforms of arterial dimensions

Ultrasonic PT, which has superior measurement accuracy compared with the phase-locked echo tracking system (Hasegawa and Kanai 2006), was newly employed in the present study to measure pulse waveforms of arterial dimensions in the fetal period. D_{min} and D_{max} increased linearly with gestational age; however, DID had a negative squared correlation. DID exhibited a rapid increase before 28 wk, but the rate of increase subsequently slowed until no further increase was observed, suggesting an increase in cardiac stroke volume or PP occurs during the fetal period. Sugawara et al. (2000) reported a positive linear relationship between pulse pressure and the internal diameter of human arteries. This previous finding indicates that the increases in D_{min}, D_{max} and DID with gestational age reflect a developmental rise in systolic, diastolic and pulse pressures, respectively. The CV and ICC in measurements are thought to be acceptable, as they seem to be on the same level as those from Doppler examinations or speckle tracking for fetal cardiovascular investigation (Mavrides et al 2001; Van Mieghem et al. 2010). Bland–Altman analysis revealed no systematic inter-observer errors in these measurements.

It has been recognized that both structural development and functional development of the myocardium occur during the fetal and neonatal periods. In the fetal myocardium, only relatively small numbers of sarcoplasmic reticuli, transverse tubules and mitochondria are present, and only limited ATPase activity is observed (Brook et al. 1983; Ingwall et al. 1981; Nakanishi et al. 1986, 1987). Several studies have investigated calcium channels in fetal cardiomyocytes, which provide myocardial contractility (Nguemo et al. 2007; Wetzel et al. 1993). L-Type Ca^{2+} currents exhibit rapid increases during the fetal period, especially during the first half (Masuda et al. 1995), that may explain the plateau in DID after 28 wk. However, few details of increasing fetal arterial function are known; nonetheless,

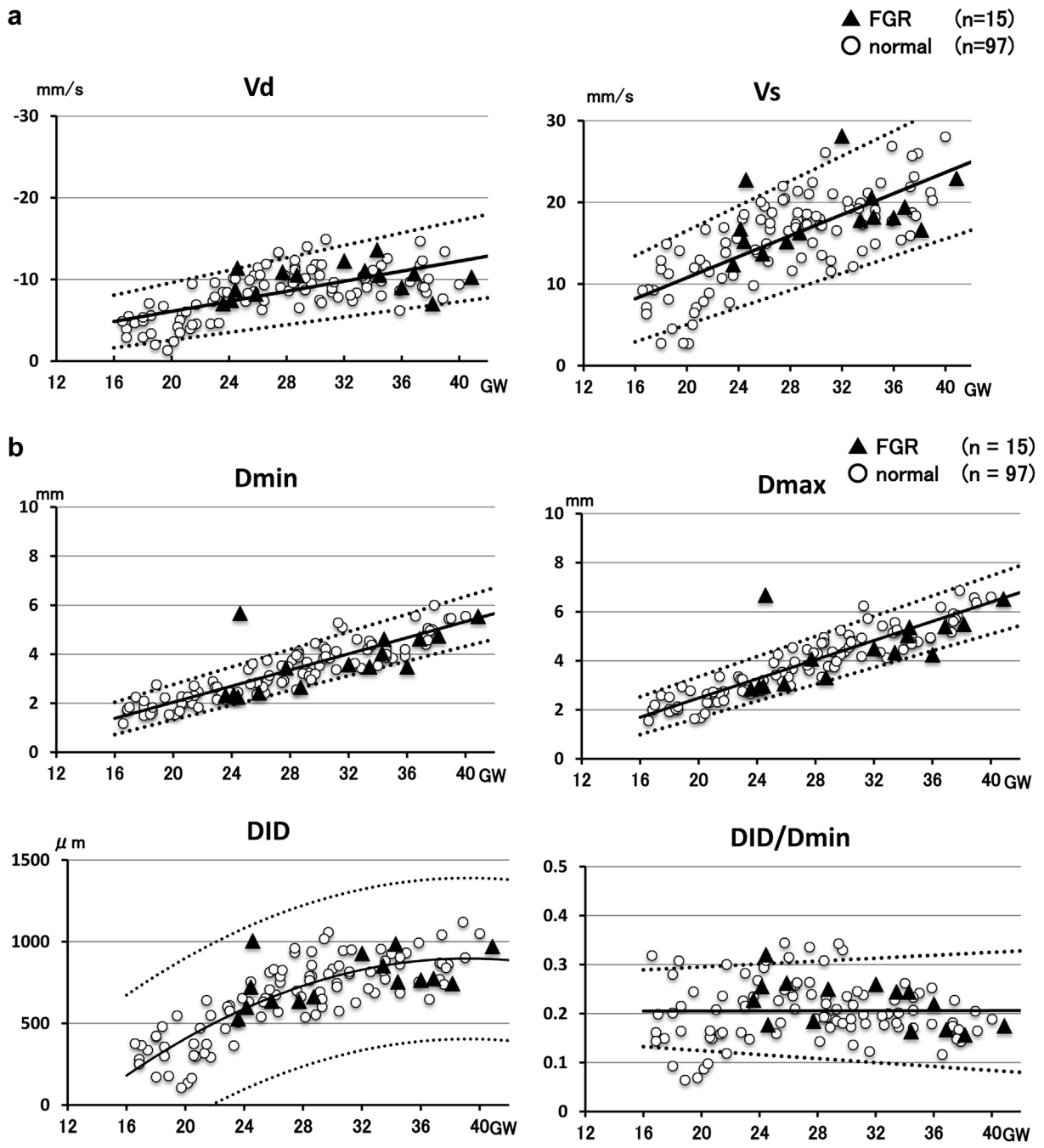

Fig. 4. (a) V_d and V_s in relation to gestational week in normal and growth-restricted fetuses. The *solid line* represents the regression line, and the *dotted lines* indicate the 95% confidence interval. (b) D_{min}, D_{max}, DID and DID/D_{min} in relation to gestational week in normal and growth-restricted fetuses. The *solid line* represents the regression line, and the *dotted lines* indicate the 95% confidence interval. FGR = fetal growth restriction; GW = gestational week.

this structural and functional development in the myocardium may explain the increases in blood pressure as relating to D_{min}, D_{max} and DID of the arterial pulse waveform. After establishment of a developmental pattern for D_{min}, D_{max}, DID and DID/D_{min} in normally growing fetuses, we found no statistical differences between the two study groups in relation to these parameters, suggesting minimal or concealed changes in internal diameter occurred in the growth-restricted fetuses relative to the normal fetuses during the fetal period.

Pulse wave velocity

Measurement of PWV is a well-established method for the non-invasive evaluation of arterial stiffness after

Table 2. Results of regression analysis for normally developing fetuses and two-way ANOVA for growth-restricted fetuses

Parameter	Estimated equation	Regression analysis		Two-way ANOVA: normal vs. FGR
		R^2	*p*-value	*p*-value
V_d (mm/s)	$-0.31 \times GW + 0.074$	0.43	<0.001	0.42
V_s (mm/s)	$0.65 \times GW - 2.13$	0.55	<0.001	0.60
D_{min} (mm)	$0.17 \times GW - 1.25$	0.84	<0.001	0.73
D_{max} (mm)	$0.20 \times GW - 1.44$	0.87	<0.001	0.98
DID (μm)	$1.33 \times GW^2 + 104 \times GW - 1148$	0.70	<0.001	0.20
DID/D_{min}	$0.00005 \times GW + 0.204$	0.000030	0.76	0.13
PWV (m/s)	$0.0018 \times GW + 1.73$	0.0043	0.098	<0.001
Estimated PP (kg m^{-1} s^{-2})	$0.0025 \times GW + 2.46$	0.00015	0.93	<0.001

ANOVA = analysis of variance; DID = difference in internal dimensions; FGR = fetal growth restriction; GW = gestational week; PP = pulse pressure; PWV = pulse wave velocity.

birth. Positive correlation of PWV with mean blood pressure was also reported in adult patients (Stewart et al. 2003). However, to date, only a few studies have attempted to measure fetal PWV. In the present study, we employed the phased-tracking method to measure fetal local PWV in normal and growth-restricted fetuses. Intra-observer and inter-observer reliabilities were thought to be acceptable in this study (Table 3).

Traditionally, PWV has been measured at the time of transit of the foot of the pressure or displacement wave and not the peak derivative of pressure. The foot of the pressure wave is not affected by reflected waves, which makes the positions of the peaks in pressure and its derivative change with respect to the foot because of the backward moving waves; therefore, PWV changes during the cardiac cycle and depends on diastolic pressure. However, in the present study, changes in the diameters of some waves were difficult to measure because of the uncertainty of the bottom point of the fetal cardiac cycle. We decided, instead, to use velocity waves with clear peaks. The differences were thought to be small because the measurement sites were close and the peak velocity occurred very close to the foot of displacement and was minimally affected by reflections. Five serial waves were analyzed, and their average was employed in this study. In all cases, five serial waves were almost the same in its figure and time scale, and we could not point out significant differences among the waves in the same case. We thought it sufficient to measure velocity waves to evaluate fetal PWV even though the systolic and diastolic phases could not be distinguished accurately.

Fetal PWV was typically around 2 m/s and exhibited a slight elevation during the fetal period, which is lower than the range of 4–8 m/s reported for healthy children and young adults (Koivistoinen et al. 2007; Reusz et al. 2010), suggesting low arterial stiffness or low pulse pressure in the fetal period. In the present study, elevated PWV was observed in growth-restricted fetuses, which can likely be explained by the alteration of arterial wall properties. Several studies have focused on the structural remodeling of arterial walls in growth-restricted fetuses in animal models and human patients. In particular, the elastin-versus-collagen ratio has been reported to be a major determinant of arterial stiffness (O'Rourke et al. 2002), and increased collagen content has been reported to provide a good measure of the decrease in compliance of arterial walls (Dodson et al. 2013; Thompson et al. 2011). Further, Kinzler et al. (2005) reported that the mRNA of collagen I and III was increased in the cord blood of growth-restricted fetuses, and a negative relation between arterial stiffness and birth weight has been observed (Cheung et al. 2004). However, there is no evidence of increased diastolic pressure in the fetal period, even in animal models of growth restriction.

Various investigators have described a prenatal programming effect on blood pressure. Prenatal hyponutrition or hypoxia results in small numbers of nephrons, which is a strong predictor of adult hypertension (Ritz et al. 2011). Liao et al. (1999) reported that decreased arterial stiffness is related to the development of hypertension in normotensive patients. Low birth weight is

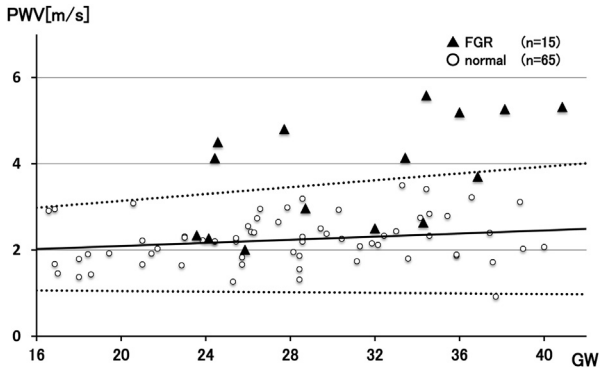

Fig. 5. Pulse wave velocity in relation to gestational week in normal and growth-restricted fetuses. The *solid line* represents the regression line, and the *dotted lines* indicate the 95% confidence interval. FGR = fetal growth restriction; GW = gestational wk; PWV = pulse wave velocity.

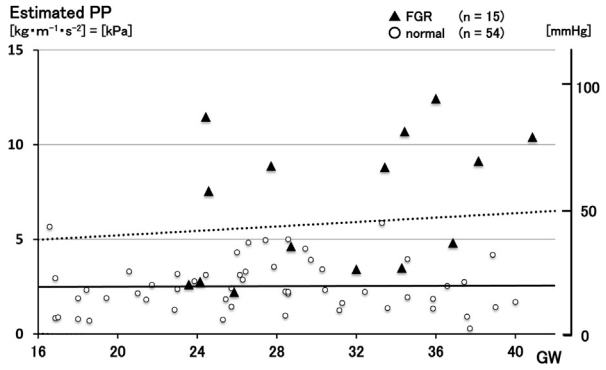

Fig. 6. Estimated pulse pressure in relation to gestational week in normal and growth-restricted fetuses. The *solid line* represents the regression line, and the dotted lines indicate the 95% confidence interval. FGR = fetal growth restriction; GW = gestational wk; PP = pulse pressure.

reported to be associated with increased stiffness of large arteries and reduced compliance and with increased blood pressure in adult life (Martyn et al. 1995). Thus, fetal PWV measurement may be helpful in the early recognition of persons with a high risk of adult-onset hypertensive diseases.

Estimated pulse pressure

Struijk et al. (1992, 2013) reported on the estimation of fetal PP; however, an echo-tracking system was employed for measurements of the diameter of the descending aorta. In the present study, we could analyze data from a sufficient number of individuals with the superior measurement accuracy of PT. Nonetheless, the estimated PP values were around 2.5 kPa (19 Torr), which seemed too high, and the values varied widely in normal fetuses, but were typically less than 5 kPa in most cases. These results indicate our estimation model is not appropriate and requires further modification. Several reasons could account for the high values. A non-linear relationship between pressure and compliance can be assumed with a very low pressure range in an actual fetal descending aorta. The circumferential elastic modulus (E_θ) was taken into account in the Moens–Korteweg equation, but the radial and axial elastic moduli might be the causes of non-linearity. The fetal descending aorta is bound firmly on the dorsal side, which could have resulted in asymmetric wall motion and thereby affected PWV. In addition, estimated PP assumed a constant PWV, but PWV changes during the cardiac cycle. Finally, the fetal body is inside the amniotic cavity. As such, it remains controversial whether intrauterine static pressure can be ignored and whether blood pressure functions the same way as *ex utero*.

The estimated PP was elevated in growth-restricted fetuses in the present study. There was no clear evidence of enlarged arteries in growth-restricted fetuses in the same gestational week; therefore, estimated PP was thought to represent fetal PP, but the absolute values were nonetheless too high. However, estimated PP might be used as an index of fetal PP and could be sufficient for ontogenic evaluation. A future direction of this study will be to use PWV and estimated PP to relate blood pressure to fetal compromise in, for example, structural heart diseases, arrhythmia and twin-to-twin transfusion syndrome.

Study limitations

This study had several limitations. First, calibration of blood pressure is quite difficult in fetuses. Second, there was no conclusive proof of a linear relation between pressure and internal diameter in the low pressure range in fetuses during early gestation. Third, the initial points at which to begin tracking on the arterial wall were set manually in our system. Hence, the spatial resolution of the initial internal diameter depended on the fundamental transmission frequency in the B-mode of the ultrasound instrument. Also, the temporal resolution of 2.38 ms was fair, but not quite sufficient for estimating PWV. Finally, the method used to measure PWV differed from that commonly used in infants or adolescents because arterial tonometry is almost impossible in the

Table 3. Intra- and inter-observer reliability of measurements in phased-tracking method

Parameter	Number of patients	Number of measurements	Coefficient of variation (%)	Intra-class correlation coefficient	Bland–Altman analysis	
					Pairs of measurements	*p*-value*
V_d	68	340	6.4 ± 0.46†	0.90	74	0.58
V_s	68	340	4.8 ± 0.38	0.93	74	0.48
D_{min}	69	345	6.3 ± 0.42	0.95	74	0.79
D_{max}	69	345	5.0 ± 0.33	0.96	74	0.80
DID	56	280	5.4 ± 0.56	0.95	74	0.39
PWV	53	265	9.3 ± 0.87	0.95	58	0.91

DID = difference in internal dimensions; PWV = pulse wave velocity.
* *p*-Value for significant difference in average of measurements.
† Mean ± standard error.

fetal period. In the future, improved spatial and temporal resolution will enable direct measurement of foot-to-foot of displacements, which will facilitate accurate measurements of PWV, especially for the small distance in tiny fetuses.

CONCLUSIONS

The ultrasonic phased-tracking method was found to be feasible for evaluating the dimensions and PWV of the fetal descending aorta with fair accuracy. It was possible to estimate fetal PP with the Moens–Korteweg equation, but this estimation model was found to be incomplete and will require further modifications to be suitable for fetuses.

REFERENCES

Brook WH, Connell S, Cannata J, Maloney JE, Walker AM. Ultrastructure of the myocardium during development from early fetal life to adult life in sheep. J Anat 1983;137(Pt 4):729–741.

Cheung YF, Wong KY, Lam BC, Tsoi NS. Relation of arterial stiffness with gestational age and birth weight. Arch Dis Child 2004;89:217–221.

Dodson RB, Rozance PJ, Fleenor BS, Petrash CC, Shoemaker LG, Hunter KS, Ferguson VL. Increased arterial stiffness and extracellular matrix reorganization in intrauterine growth-restricted fetal sheep. Pediatr Res 2013;73:147–154.

Fujita Y, Satoh S, Koga T, Mori A, Nakano H. Aortic pulse waveforms for evaluating cardiac performance in the human fetus. Ultrasound Med Biol 2002;28:1245–1250.

Gennser G, Isberg PE. Interdependence of pulse wave variables in the human fetal aorta. J Biomed Eng 1987;9:54–58.

Hasegawa H, Kanai H. Modification of the phased-tracking method for reduction of artifacts in estimated artery wall deformation. IEEE Trans Ultrason Ferroelectr Freq Control 2006;53:2050–2064.

Hinghofer-Szalkay H, Greenleaf JE. Continuous monitoring of blood volume changes in humans. J Appl Physiol 1987;63:1003–1007.

Hokanson DE, Mozersky DJ, Sumner DS, Strandness DE Jr. A phase-locked echo tracking system for recording arterial diameter changes in vivo. J Appl Physiol 1972;32:728–733.

Hokanson DE, Strandness DE Jr, Miller CW. An echo-tracking system for recording arterial-wall motion. IEEE Trans Sonics Ultrason 1970;SU-17:130–132.

Ingwall JS, Kramer MF, Woodman D, Friedman WF. Maturation of energy metabolism in the lamb: Changes in myosin ATPase and creatine kinase activities. Pediatr Res 1981;15:1128–1133.

Kanai H, Sato M, Koiwa Y, Chubachi N. Transcutaneous measurement and spectrum analysis of heart wall vibrations. IEEE Trans Ultrason Ferroelectr Freq Control 1996;43:791–810.

Kinzler WL, Smulian JC, Kistler CA, Hahn RA, Zhou P, Gordon MK. Extracellular matrix changes in the umbilical arteries of growth-restricted fetuses. Am J Obstet Gynecol 2005;192:1053–1059.

Koivistoinen T, Kööbi T, Jula A, Hutri-Kähönen N, Raitakari OT, Majahalme S, Kukkonen-Harjula K, Lehtimäki T, Reunanen A, Viikari J, Turjanmaa V, Nieminen T, Kähönen M. Pulse wave velocity reference values in healthy adults aged 26–75 y. Clin Physiol Funct Imaging 2007;27:191–196.

Liao D, Arnett DK, Tyroler HA, Riley WA, Chambless LE, Szkio M, Heiss G. Arterial stiffness and the development of hypertension: The ARIC study. Hypertension 1999;34:201–206.

Luterkort M, Gennser G. Cardiovascular dynamics in relation to presentation and postural changes in normal fetuses. Eur J Obstet Gynecol Reprod Biol 1987;24:13–22.

Martyn CN, Barker DJ, Jespersen S, Greenwald S, Osmond C, Berry C. Growth in utero, adult blood pressure, and arterial compliance. Br Heart J 1995;73:116–121.

Masuda H, Sumii K, Sperelakis N. Long openings of calcium channels in fetal rat ventricular cardiomyocytes. Pfluegers Arch 1995;429:595–597.

Mavrides E, Holden D, Bland JM, Tekay A, Thilaganathan B. Intra-observer and inter-observer variability of transabdominal Doppler velocimetry measurements of the fetal ductus venosus between 10 and 14 wk of gestation. Ultrasound. Obstet Gynecol 2001;17:306–310.

Mori A, Iwabuchi M, Makino T. Fetal haemodynamic changes in fetuses during fetal development evaluated by arterial pressure pulse and blood flow velocity waveforms. BJOG 2000;107:669–677.

Nakanishi T, Nagae M, Takao A. Developmental changes in contractile protein adenosine 5'-triphosphatase in the rabbit heart. Circ Res 1986;58:890–895.

Nakanishi T, Okuda H, Kamata K, Abe K, Sekiguchi M, Takao A. Development of myocardial contractile system in the fetal rabbit. Pediatr Res 1987;22:201–207.

Nguemo F, Fleischmann BK, Schunkert H, Hescheler J, Reppel M. Functional expression and inactivation of L-type Ca^{2+} currents during murine heart development—Implications for cardiac Ca^{2+} homeostasis. Cell Physiol Biochem 2007;20:809–824.

Niki K, Sugawara M, Chang D, Harada A, Okada T, Sakai R, Uchida K, Tanaka R, Mumford CE. A new non-invasive measurement system for wave intensity: Evaluation of carotid arterial wave intensity and reproducibility. Heart Vessels 2002;17:12–21.

O'Rourke MF, Staessen JA, Vlachopoulos C, Duprez D, Plante GE. Clinical applications of arterial stiffness: Definitions and reference values. Am J Hypertens 2002;15:426–444.

Reusz GS, Cseprekal O, Temmar M, Kis E, Cherif AB, Thaleb A, Fekete A, Szabó AJ, Benetos A, Salvi P. Reference values of pulse wave velocity in healthy children and teenagers. Hypertension 2010;56:217–224.

Ritz E, Amann K, Koleganova N, Benz K. Prenatal programming: Effects on blood pressure and renal function. Nat Rev Nephrol 2011;7:137–144.

Sabbah HN, Marzilli M, Stein PD. The relative role of subendocardium and subepicardium in left ventricular mechanics. Am J Physiol 1981;240:H920–H926.

Sindberg Eriksen P, Gennser G. Acute responses to maternal smoking of the pulsatile movements in fetal aorta. Acta Obstet Gynecol Scand 1984;63:647–654.

Stale H, Marsal K, Gennser G, Benthin M, Dahl P, Lindström K. Aortic diameter pulse waves and blood flow velocity in the small, for gestational age, fetus. Ultrasound Med Biol 1991;17:471–478.

Stewart AD, Millasseau SC, Kearney MT, Ritter JM, Chowienczyk PJ. Effects of inhibition of basal nitric oxide synthesis on carotid–femoral pulse wave velocity and augmentation index in humans. Hypertension 2003;42:915–918.

Struijk PC, Migchels H, Mathews JV, Stewart PA, Clark EB, de Korte CL, Lotgering FK. Fetal aortic distensibility, compliance and pulse pressure assessment during the second half of pregnancy. Ultrasound Med Biol 2013;39:1966–1975.

Struijk PC, Wladimiroff JW, Hop WC, Simonazzi E. Pulse pressure assessment in the human fetal descending aorta. Ultrasound Med Biol 1992;18:39–43.

Sugawara M, Niki K, Furuhata H, Ohnishi S, Suzuki S. Relationship between the pressure and diameter of the carotid artery in humans. Heart Vessels 2000;15:49–51.

Thompson JA, Gros R, Richardson BS, Piorkowska K, Regnault TR. Central stiffening in adulthood linked to aberrant aortic remodeling under suboptimal intrauterine conditions. Am J Physiol Regul Integr Comp Physiol 2011;301:R1731–R1737.

Van Mieghem T, Giusca S, DeKoninck P, Gucciardo L, Done E, Hindryckx A, D'Hooge J, Deprest J. Prospective assessment of fetal cardiac function with speckle tracking in healthy fetuses and recipient fetuses of twin-to-twin transfusion syndrome. J Am Soc Echocardiogr 2010;23:301–308.

Wetzel GT, Chen F, Klitzner TS. Ca^{2+} channel kinetics in acutely isolated fetal, neonatal, and adult rabbit cardiac myocytes. Circ Res 1993;72:1065–1074.